

We are IntechOpen, the world's leading publisher of Open Access books Built by scientists, for scientists

6,900

Open access books available

186,000

International authors and editors

200M

Downloads

Our authors are among the

154

Countries delivered to

TOP 1%

most cited scientists

12.2%

Contributors from top 500 universities



WEB OF SCIENCE™

Selection of our books indexed in the Book Citation Index
in Web of Science™ Core Collection (BKCI)

Interested in publishing with us?
Contact book.department@intechopen.com

Numbers displayed above are based on latest data collected.
For more information visit www.intechopen.com



Stimulated Raman Scattering in Micro- and Nanophotonics

Maria Antonietta Ferrara and Luigi Sirleto

Abstract

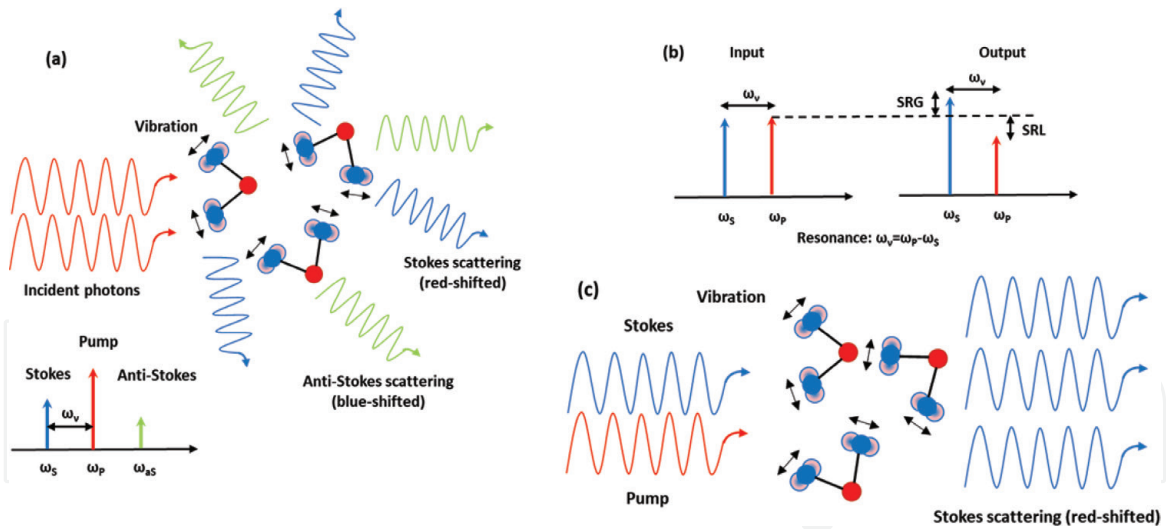
Micro- and nanophotonics explore behavior of light on the micro-/nanoscale and the interaction of micro-/nanoobjects with light. The driving force for their development is the aim to go beyond the limit of photonics. Because of the diffraction limit, photonics components are not able to confine light to the microscale or nanoscale dimension; therefore, one of the key challenges for micro- and nanophotonics is a reduction in the size of integrated optical devices, while maintaining a high level of performance. As far as light amplifiers and laser sources based on stimulated Raman scattering (SRS) are concerned, important accomplishments have been achieved in the fields of fiber optics amplification and integrated photonics devices. In this chapter, the most interesting investigations in the field of stimulated Raman scattering in micro- and nanophotonics are reviewed. These findings provide promising perspectives for integrated micro-/nano-Raman lasers.

Keywords: nonlinear optics, stimulated Raman scattering, Raman laser, microphotonics, nanomaterials, nanophotonics

1. Introduction

Spontaneous Raman is an inelastic light scattering by which a fraction of the light incident upon a transparent material is shifted in frequency. Linear Raman scattering is a weak process (approximately 1 in 10^7 photons) involving the collective behavior of many atoms, behaving independently (see **Figure 1(a)**) and leading to nearly isotropic emission. Raman spectra, given by the superposition of stochastic totally independent vibrations from individual molecules, are unique to the material [1].

Stimulated Raman scattering (SRS) phenomenon occurs when there is a transfer of energy from a high power pump beam to a probe beam (copropagating or counterpropagating) through SRS. In particular, this energy exchange occurs when the frequency difference between the pump and the Stokes laser beams matches a given molecular vibrational frequency of the sample under test; the SRS effect occurs in the form of a gain of the Stokes beam power (stimulated Raman gain, SRG) and a loss of the pump beam power (stimulated Raman loss, SRL. See **Figure 1(b)**) [2]. Because of its coherent nature, the molecular bonds oscillate in phase and interfere constructively inside the focus area of the laser beam. As a consequence a SRS signal, which is orders of magnitude bigger than spontaneous Raman scattering, is generated (about 20–30% of the incident laser radiation can efficiently be converted into SRS) (see **Figure 1(c)**).


Figure 1.

(a) Spontaneous Raman scattering: incident photons inelastically scatter off spontaneously from vibrationally excited molecules, behaving independently. (b) Stimulated Raman scattering: two incident lights, a pump and a Stokes laser beams, whose energy difference matches a particular vibrational energy, drive the molecule at $\omega_v = \omega_s - \omega_p$ producing coherent Raman signals at $\omega_s = \omega_p + \omega_v$. SRS modalities are: SRG, stimulated Raman gain; SRL, stimulated Raman loss. (c) Stimulated Raman scattering: inelastic scattering of probe photons off from vibrationally excited molecules that interfere coherently.

Due to its Raman-shifted output, SRS is a workable method for generating coherent radiation at new frequencies. SRS permits, in principle, the amplification in a wide interval of wavelengths, from the ultraviolet to the infrared. Since the Raman frequency of a medium is usually fixed, the tunability can be achieved by using a tunable pump laser. Raman lasing occurs when the Raman-active gain medium is placed between mirrors, reflecting the first Stokes wavelength. This is analogous to lasers, where the gain medium must be placed inside a cavity to achieve laser threshold. Raman lasers and traditional lasers differ in the wavelength of light required for pumping. In the case of Raman laser, it does not depend on the electronic structure of the medium, so the wavelength of pump laser can be chosen to minimize absorption.

In order to tailor Raman laser characteristics and performances, there are two main basic configurations. The first one, external-resonator Raman laser, the Raman crystal is placed inside a cavity, resonating the Stokes field (**Figure 2(a)**). This configuration is used for pump pulses that are longer than the transit time through the Raman crystal. The second one, the intracavity Raman laser (**Figure 2(b)**) combines both a Raman medium and the laser medium inside a single cavity, so that the fundamental and Stokes fields are both resonating within the cavity [3].

Raman amplification, demonstrated in the early 1970s, is a feasible approach for fiber optics amplification, being only restricted by the pump wavelength and Raman active modes of the gain medium [4]. In this case, optical fiber is used as Raman gain medium and both pump and signal waves are launched into it (**Figure 2(c)**). In the past century, fused silica has been the main material used for transmission of optical signals, because of its good optical properties and attractive trade-off between Raman gain and losses. The main disadvantage of the current silica fiber amplifiers is the limited usable bandwidth for Raman amplification (5 THz, approx. 150 cm^{-1}). A development in fiber optics communications was achieved opening the communication range to span from 1270 to 1650 nm, corresponding to about 50 THz bandwidth [5]. For future amplification requirements, due to this significant increase in bandwidth, the use of existing Er-doped fiber amplifiers is kept out, while Raman gain becomes the key mechanism.

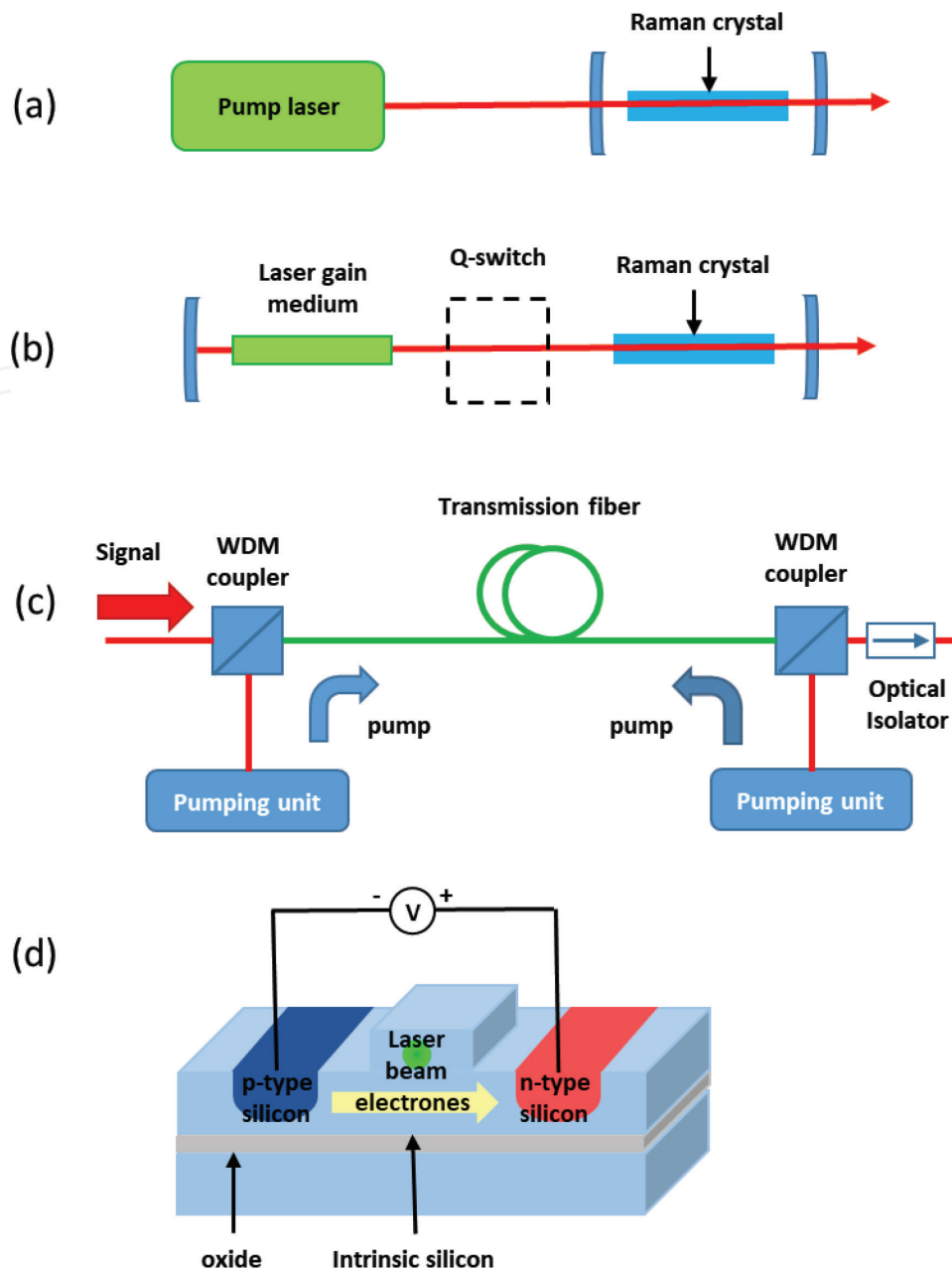


Figure 2. Basic configurations of Raman laser: (a) external-resonator Raman laser; (b) intracavity Raman laser; (c) fiber Raman amplifiers; and (d) silicon on insulator waveguide Raman laser.

Silicon photonics is an important player in the low-cost optical interconnect technology, as silicon-based optical components could be manufactured using the existing silicon fabrication techniques [6]. Silicon on insulator (SOI) waveguides allows to limit the optical field into an area 100 times smaller than the modal area of a typical single-mode optical fiber. In addition, the Raman gain in silicon is much stronger than in glass ($\approx 10,000$ times), therefore allowing to reduce the length required from kilometers of fiber to centimeters of silicon waveguides [2]. The waveguide approach, schematically reported in **Figure 2(d)**, led to the demonstration of pulsed Raman silicon laser [7] and continuous-wave (CW) lasing [8]. The merit of this approach is the ability to use pure silicon without the need for Er doping; i.e. it is fully compatible with silicon microelectronics manufacturing. On the other hand, there are three main limitations. The first, Raman laser cannot be electrically excited and it requires an off-chip pump. The second, the narrow-band (105 GHz) of stimulated Raman gain makes it unsuitable for its use in WDM applications, unless expensive multi-pump schemes are implemented. The third,

Raman gain in Si at the wavelength of interest for telecommunications is reduced by two-photon absorption (TPA).

We note that as a general rule, in all laser gain bulk materials there is a tradeoff between gain and bandwidth: linewidth may be increased at the expense of peak gain. In nature, we have material with high Raman gain and small bandwidth (for example, silicon), and others with a large bandwidth but with small Raman gain (for example, silica). This trade-off is a fundamental limitation toward the realization of sources with high efficiency and large emission spectra. In this book chapter, a review of the most significant accomplishments in the field of SRS in micro- and nanophotonics is reported. From a theoretical point of view, the difference between micro- and nanostructures is significant. In microstructures, the measured SRS enhancement can be related to photons confinements effect and it can be quantified by a corresponding gain (g_{micro}), given by: $g_{micro} = f^* g_{bulk}$, where f is the optical field enhancement due to the presence of microstructures and g_{bulk} is the gain of bulk material, making up the microstructures [2]. According to this formula, photonics microstructures allow an enhancement of Raman gain, but the bandwidth does not change, therefore the fundamental trade-off between gain and bandwidth of bulk materials cannot be overcome using microstructures. Concerning SRS in nanostructures, although a general theory on the relation between nanostructuring and Raman gain is not established, we expect that the Raman gain of nanomaterials g_{nano} should be related to the intrinsic properties of materials and for this reason different from bulk. Therefore, the fundamental trade-off between gain and bandwidth should be overcome, too.

The chapter is organized as follows. In Section 2, some the most successful applications areas of SRS in microstructures are described. In Section 3, a number of investigations concerning SRS in nanostructures are described. Finally, in the appendix, for the sake of completeness, the basic theory of SRS and experimental methods for measuring Raman gain are reported.

2. SRS in microphotonics

In this section, in order to describe stimulated Raman scattering investigations in microstructures, two crucial parameters have been individuated: dimension of microstructure and order/disorder degree of microstructure distribution. As to regard dimension of microstructure, in order to point out its role, in Section 2.1, SRS investigations in microcavities are reported. Concerning the order/disorder degree of microstructure distribution, we note that interesting developments have been recently demonstrated, which point out that it is possible to make use of the intrinsic order/disorder in photonic materials to create useful optical functionality [9]. In order to highlight the role of order/disorder degree of microstructure distribution, we describe two limit cases: in Section 2.2 SRS in photonics crystals, i.e. in a completely ordered structure, is reported, while in Section 2.3 SRS in random laser, i.e. in a disordered structure is described.

2.1 SRS in microcavities

In nonlinear optics devices, the use of microcavities allows to take advantage of both the micrometers dimension and the increasing of the local field, combining small modal volume with high optical quality-factors (Q). One of the most important consequences for nonlinear optics applications is that strong resonant increase of energy in microscale volumes significantly reduces the power threshold at which nonlinear optical effects occur [10]. In the case of SRS, in agreement with the observed SRS for high- Q cavities experimental results [10], the explicit

expression of the cavity-enhanced Raman gain shows that the improvement is inversely proportional both to the square of the radius of the spherical cavity and to the linewidth of the Raman process.

In Ref. [11], SRS from spherical droplets and microspheres, with diameters of the order of tens of micrometers and optically coupled by the use of a tapered optical fiber, has been observed. The threshold was measured whereas the coupling air gap between the taper and microsphere was changed, allowing to obtain a micrometer-scale, nonlinear Raman source with a pump threshold approximately 1000 times lower than reported before and a pump-signal conversion higher than 35% [2, 11].

Diamond as a possible material for compact, on-chip Raman lasers over a wide spectrum was introduced in Ref. [12]. A CW, low-threshold, tunable Raman laser operating at $\sim 2 \mu\text{m}$ wavelengths based on waveguide-integrated diamond racetrack microresonators embedded in silica on a silicon chip was demonstrated.

2.2 SRS in photonics crystals

A high-quality-factor nanocavity using a photonic crystal with a triangular lattice structure realized by circular air holes in a suspended silicon membrane and without any p-i-n diodes, yielding a device with a cavity size of less than $10 \mu\text{m}$, has been demonstrated in Ref. [13]. The heterostructure nanocavity is obtained by introducing a line defect waveguide with two kinds of propagation modes inside the photonic bandgap, an odd-waveguide mode and an even-waveguide mode, which were used to confine pump light and Stokes-Raman-scattered light, respectively. A continuous-wave Raman silicon laser with an extraordinary low lasing threshold of $1 \mu\text{W}$ was demonstrated. In fact, an optimized nanocavity design allows to produce a net Raman gain in the low-excitation range before TPA-induced free carrier absorption (FCA) becomes dominant, permitting a low lasing threshold [2, 13].

2.3 SRS in random laser

Multiple scattering is a well-known phenomenon, occurring in nearly all optical opaque materials. Random walk of light waves in disordered materials could carry out to a multiple scattering with a consequent strong localization of electric field. Wave character of multiply scattered light is not lost and the wave can interfere both during and after the scattering process. Considering that the scattering is elastic, optical information does not change. Furthermore, due to reciprocity, multiple scattering is, in theory, fully reversible [2]. Reciprocity means that waves following the same path in opposite directions can interfere. Interference between such counter-propagating waves is always constructive, which gives rise to the incredibly robust interference phenomenon of coherent backscattering (also called weak localization). The combination of weak localization together with reciprocity, leads to a series of interesting physical effects and to an enormous potential for new disorder-based optical applications [14].

The first experimental evidence of lasing via a Raman interaction in a bulk three-dimensional random medium was demonstrated taking advantage of barium sulfate (BaSO_4) powder with particle diameters of $1\text{--}5 \mu\text{m}$. The pump energy threshold was 1.05 mJ ; at higher values, gain is stronger than losses and SRS dominates the conversion process, allowing to obtain random Raman lasing. A Raman signal of 2.0 mJ was measured at a maximum of 11.5 mJ of pump energy [2, 15]. The complicated dynamics of nonlinear pulse propagation in a turbid medium make a theoretical approach to describing this problem very challenging.

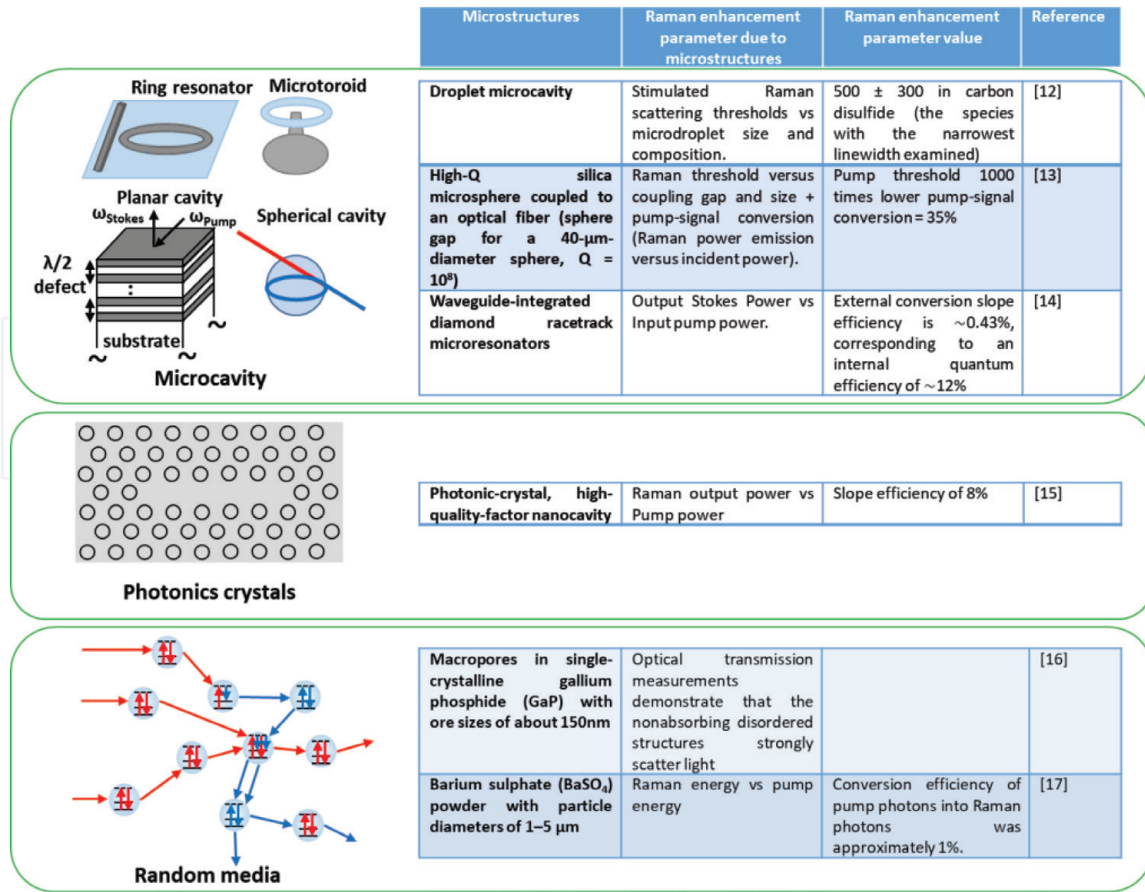


Figure 3. SRS enhancement reported in different kind of microstructures.

To have a rapid idea of the Raman enhancement reported by the different approaches in microstructures described in this section, in **Figure 3** we summarized them.

3. SRS in nanophotonics

In order to control a signal light, its intensity or phase has to be modified by a control signal. In a nonlinear optics device, a control light-wave is employed to modify the optical properties of the medium as seen by a signal light-wave. Of course, higher nonlinearity requires shorter interaction length L . In order to reduce L in a nonlinear device with physical dimensions greater than the wavelength, the efficiency of nonlinear effects can be enhanced taking advantage of optical resonators (see Section 2.1 for examples) [2]. In nanoscale devices, which should be able to control light with light in a nanoscale layer or in a nanoparticle of nonlinear material, the trick of using optical resonators cannot be used. Therefore, we have to develop nanostructured materials having enough large nonlinearities [16].

The search for new materials, from an experimental point of view, should satisfy a number of technological and economical requirements, while, from a theoretical point of view, it should be combined with a deep understanding of nonlinear polarization mechanisms, elucidating their relation to the structure of nanostructures (average radius, volume fraction and size dispersions) [17]. In the past few decades, a number of nanomaterials proved remarkable nonlinear optical (NLO) properties, which encourage the fabrication of ultra-compact, low-loss and high-performance nanoscale photonic devices [18].

Recent interest in the optical responses of metal nanoparticles and metamaterials is focused on enhancing local electromagnetic fields [19]. The significant enhancement factors of 10^3 – 10^6 , predicted at a flat metal surface, are significant for nonlinear optical processes [19]. However, although plasmonics structures and metamaterials can provide substantial size reduction for optical components, their optical losses are often undesired [20]. Therefore, in order to control the flow of light, an all-dielectric platform is highly attractive. Although *resonant nonlinearities* are significant, they are not appealing for applications, due to their long response times. In addition, at resonance the incident radiation is absorbed by materials [17]. On the other hand, *nonresonant nonlinearities* take place at frequencies below the absorption edge (i.e. when the light linear absorption is negligible) and they are very fast (typical recovery times are of the order of picoseconds). Recently, third-order NLO properties of Si-nc have been widely investigated and a large variation of the nonlinear refractive index (n_2) values has been reported, complicating the interpretation of experimental results [21].

As far as the investigation of SRS at the nanoscale is concerned, there have been a few number of fundamental investigations, both experimental and theoretical. In Ref. [22], a large Raman gain, measured by resonant Raman spectra excited at 632.8 nm, was obtained from individual single-walled carbon nanotubes. The theoretical interpretation takes in to account both the exceptional nonlinear properties and the efficient electron-phonon interaction in single-walled carbon nanotubes. In Ref. [23], SRS from GaP nanowires was measured by Raman spectra in backscattering configuration, using CW laser excitation (514.5 nm). Strong nonlinear SRS, obtained by crystalline nanowires with a diameter of 210 nm and with length of about 1 micron, were discussed in terms of theoretical results developed for dielectric cavities.

In the following, the observation of SRS in nanostructured silica-based materials (Section 3.1) and nanostructured silicon-based materials (Section 3.2) are reported and discussed.

3.1 SRS in nanocomposites silica-based materials

Among the innovative materials for Raman amplification, one of the most interesting classes is oxide glasses, above all silicon dioxide-based glasses due to their compatibility with the current optical fibers technology. To try to improve their SRS efficiency, a useful strategy is to add suitable dopants (heavy metal oxides as Ta_2O_5 , Bi_2O_3 , and Nb_2O_5) to silica [24–27]. We note that in other systems, such as niobium-phosphate glasses, characterized by a high concentration of niobium, a higher peak Raman gain (but in the best case of ≈ 10 times) and a broadening of the bandwidth with respect to silica glass has been demonstrated [28, 29].

In this paragraph, in order to increase SRS optical features of silica-based glasses, we propose an alternative approach: instead of to investigate new glass compositions, we change the glass arrangement. We note that a glass structural variations can be obtained as a result of an appropriate heat treatments made in the glass transition range, generating glass-ceramics with nanocrystals uniformly dispersed in the glass matrix (glass-crystals nanocomposites) [30]. We consider glasses, belonging to the K_2O - Nb_2O_5 - SiO_2 (KNS) system, forming transparent and stable glasses and showing interesting non-linear optical properties. For glasses in the class of the KNS glass-forming system, an interesting glass nanostructuring process has been considered. The process contains two partially overlapped processes, namely, phase separation and crystallization [31]. We note that a clear relationship between glass nanostructuring and Raman gain has not been proven yet, although, in our previous paper, a connection between local structure and SRS in bulk

nanostructured $30\text{K}_2\text{O}\cdot 30\text{Nb}_2\text{O}_5\cdot 40\text{SiO}_2$ (KNS 30-30-40) glass was found [31]. It is worth noting that an appropriate choice of the annealing parameters, therefore of the degree of crystallization, can allow to obtain the best compromise between the highest Raman gain and the highest nonlinear coefficients for third order effects.

Moreover, Raman spectroscopy characterization of nanostructured $20\text{K}_2\text{O}\cdot 25\text{Nb}_2\text{O}_5\cdot 55\text{SiO}_2$ (KNS 20-25-55) glasses are also reported. The optical and structural characteristics of the samples have been measured by the Raman set up reported in Ref. [31]. Due to dependence of the intensity of the Raman active modes on both the temperature and the frequency of the vibrational modes, the measured Stokes Raman intensity was reduced according to the procedure also described in our previous papers [28–32]. Then, in order to properly compare the Raman spectra of KNS glasses with the silica glass standard, the measured Raman spectra were modified also for the differences in reflection and angle of collection by using the procedure reported in Refs. [28–32]. Usually, due to the more extended electronic clouds, elements with high atomic number yields highest intensity Raman bands, making the polarizability more sensitive to bonds stretching. Adding niobium oxide to silica-based glasses induces an enhancement of Raman cross section respect to silica glass, being the polarizability of Nb-O bonds higher than Si-O bonds. In the studied glasses, niobium enters in the glass network creating NbO_6 octahedra more or less distorted, namely with different NbO bond length, and produces several Raman bands over a wide wavenumbers range. Due to the typical glass disorder, a broadening of all Raman bands occurs and, therefore, Raman spectra of KNS glasses outcome from the strong overlapping of several broad bands.

In **Figure 4** the Raman gain respect to the Raman gain of silica is reported as a function of the Raman bandwidth for different materials. Inter alia, in **Figure 4** is evident that glasses at initial and at different times of heat-treatment show the same bandwidth, but different gain. Hence, the nanostructuring process is nearly complete in glasses at a time between 2 and 10 h and produces nanocrystalline inhomogeneities distributed in the glass matrix [30, 32].

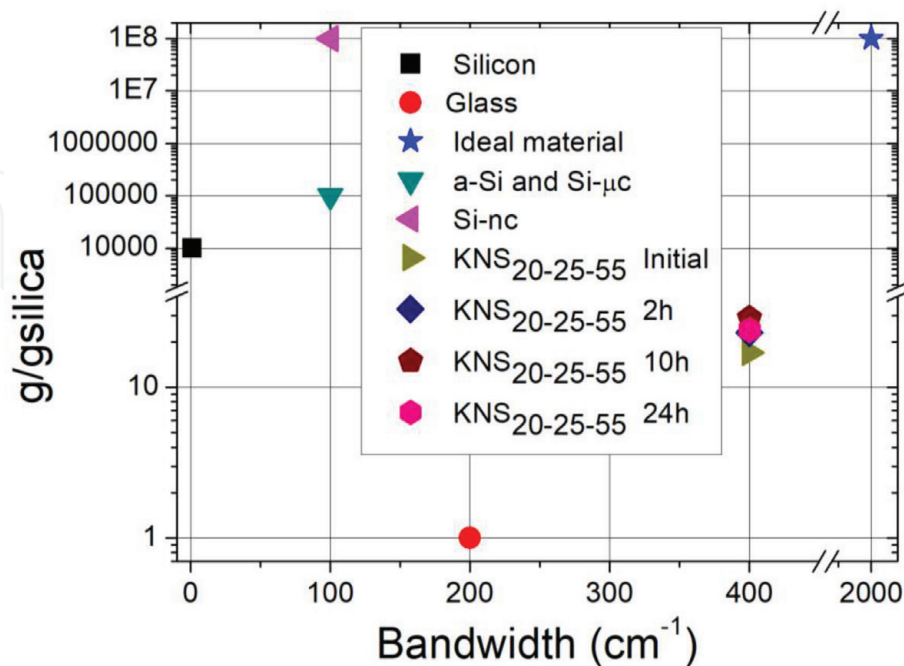


Figure 4. Raman gain coefficients and their bandwidth are reported for different material: silicon and silica (as ‘bulk material’), nanocomposite glasses (KNS) in different phases of the thermal treatment for the initial glass composition 20-25-55, silicon micro- and nano-particles (amorphous and crystalline). Features for ‘ideal materials’ for Raman amplification are reported, too.

3.2 SRS in nanostructured silicon-based materials

In our previous papers [2, 33–35] experimental results of spontaneous Raman scattering measurements in silicon nanostructures at the wavelength of interest for telecommunications (1.54 μm), were showed. Due to the phonon confinement model, two significant enhancements of the Raman spectra in silicon quantum dots respect to silicon were obtained: the broadening of spontaneous Raman emission and the tuning of the Stokes shift. In detail, in silicon quantum dots with a crystal size of 2 nm an important broadening of about 65 cm^{-1} and a peak shift of about 19 cm^{-1} were demonstrated. Taking into account that the width of C-band telecommunication is 146 cm^{-1} , we have that more than the half of C-band could be covered using silicon quantum dots, without implementing the multi-pump scheme.

In this paragraph, comparison among experimental investigations of SRS in amorphous silicon nanoparticles and in silicon micro- and nano-crystals, at the wavelengths of interest for telecommunications, are reported. We considered three different samples:

1. Silicon nanocomposites dispersed in SiO_2 matrix. The mean radius of the silicon dots and the dot density were of 49 nm and 1.62×10^8 dots/ cm^2 , respectively [36, 37].
2. Amorphous silicon nanoclusters embedded in Si-rich nitride/silicon superlattice structures (SRN/Si-SLs). The structure of the sample consists of 10 SRN layers and 9 amorphous Si (a-Si) layers for a total thickness of 450 nm. Amorphous silicon nanoclusters size was 2 nm [38–40].
3. Silicon nanocrystals (Si-nc) with a size of about 4 nm embedded in a silica matrix layer about 7 cm long. The sample was realized with an increasing concentration of Si-nc varying along the longer dimension of the sample, allowing to distinguish seven areas.

Results obtained can be summarized as follows:

- I. In silicon nanocomposites, an amplification of Stokes signal up to 1.4 dB/cm at 1542.2 nm using a 1427 nm continuous-wavelength (CW) pump laser was reported. This result demonstrates a five-fold improvement of the Raman gain respect to bulk silicon. Furthermore, a threshold power reduction of about 60% is also reported [36, 37, 40, 41].
- II. In SRN/Si-SLs, a magnification of Stokes signal up to 0.87 dB/cm at 1540.6 nm by means of a 1427 nm CW pump laser was reported. This result demonstrates a four-fold enhancement of the Raman gain with respect to bulk silicon. Additionally, a threshold power reduction of about 40% is also reported [38–41].
- III. In Si-nc an enhancement of the Raman gain by increasing their concentration was measured, and, a remarkable improvement of the Raman gain in Si-nc respect to bulk silicon, by three to four orders of magnitude depending on the Si concentration, was proven. The amplification was carried out by using a probe signal at 1541.3 nm and a pump signal at 1427 nm [2, 42, 43].

The obtained results are summarized in **Figure 4** where the Raman gain is plotted as a function of the Raman bandwidth for the considered nanostructured

silicon-based materials. By combining our earlier results on the broadening of the Raman gain spectra [33–35] with the observation of higher Raman gain [2, 36–42], bring us to state that the traditional trade-off between gain and bandwidth is overcome in low dimensional materials [30].

4. Conclusion(s)

In this book chapter, some of the most significant experimental investigations of SRS in micro- and nano-photonics are reported. The focuses are microstructures and nanostructures, which are able to enhance nonlinear interaction between light and matter based on SRS.

We try to highlight how the nonlinear interaction based on SRS can take advantage of micro- and nanostructure with respect to bulk structure in order to improve SRS efficiency. In addition, we try to discuss new perspectives for the realization of Raman lasers with ultra small sizes, which would increase the synergy between electronic and photonic devices.

A. Appendix

We note that pulsed lasers are often used in SRS experiment; therefore, we have to consider the time dependence of the output. If the pulsewidth is much longer than the relation time of the Raman excitation and the time required for light to traverse the medium, we can expect from physical argument that the output pulse will follow the temporal variation of the input pulse. This is the quasi-steady-state case. Otherwise, the output should exhibit a transient behavior. The transient effects are out of the scope of this chapter [44–46].

A.1 Theory: the classical approach

The wave equations for pump and Stokes laser pulses with electromagnetic field amplitude \vec{E}_p and \vec{E}_s at frequencies ω_p and ω_s ($\omega_p > \omega_s$), are:

$$\begin{aligned} \nabla \times (\nabla \times \vec{E}_p) - \frac{\omega_p^2}{c^2} \epsilon_p \vec{E}_p &= \frac{4\pi\omega_p^2}{c^2} \vec{P}^{(3)}(\omega_p) \\ \nabla \times (\nabla \times \vec{E}_s) - \frac{\omega_s^2}{c^2} \epsilon_s \vec{E}_s &= \frac{4\pi\omega_s^2}{c^2} \vec{P}^{(3)}(\omega_s) \end{aligned} \quad (1)$$

where $\vec{P}^{(3)}$ is the nonlinear polarizations, ϵ is the dielectric constants and c is the light velocity.

In the case of SRS, the material interaction is classically treated through a third-order nonlinear susceptibility tensor $\chi^{(3)}$ given by:

$$\chi^{(3)} = \chi^{(3)NR} + \chi^{(3)R} \quad (2)$$

which defines both electronic ($\chi^{(3)NR}$, ‘non-resonant’) and vibrational ($\chi^{(3)R}$, ‘resonant’) responses. When input laser pulse frequencies are different from electronic resonances, the first term $\chi^{(3)NR}$ does not depend on frequency, i.e. it is linked to a flat spectral background that changes immediately with the excitation change; thus, it is a real quantity. The second term, the complex quantity $\chi^{(3)R}$, characterizes the nuclear response of the molecules and yields the intrinsic vibrational mechanism of SRS [2].

In order to simplify, we study the special case of an isotropic medium with E_P and E_S with the same polarization direction and propagation along z . The whole field amplitude is: $E(z, t) = E_P e^{i(\omega_P t - k_P z)} + E_S e^{i(\omega_S t - k_S z)}$. According to Eq. (2), the nonlinear polarizations take the form:

$$\begin{aligned} P^{(3)}(\omega_P) &= [\chi_P^{(3)NR} |E_P|^2 + \chi_P^{(3)R} |E_S|^2] E_P \\ P^{(3)}(\omega_S) &= [\chi_S^{(3)R} |E_P|^2 + \chi_S^{(3)NR} |E_S|^2] E_S \end{aligned} \quad (3)$$

The $\chi_P^{(3)NR}$ and $\chi_S^{(3)NR}$ terms in $P^{(3)}$ only act to modify the dielectric constant ϵ_P and ϵ_S in Eq. (1). They are responsible for the field induced birefringence, self-focusing, etc., but have no direct effect on SRS. Therefore, in the following discussion, we neglect them. The $\chi^{(3)R}$ terms in $P^{(3)}$, instead, effectively couple E_P and E_S in Eq. (1) and is the reason of energy transfer between the two fields. They are the cause of the stimulated Raman process and are called Raman susceptibilities. Eq. (1) can be solved with Eq. (3) by knowing $\chi^{(3)R}$.

A molecular vibration or optical phonon is the most common case of SRS. The optical radiation is assumed interacting with a vibrational mode of a molecule and this vibrational mode can be defined as a simple harmonic oscillator of resonance frequency ω_0 , damping constant γ . The analysis is one-dimensional, thus, each oscillator can be distinguished by its position z and normal vibrational coordinate q [2].

The key assumption of the theory is that the optical polarizability of the molecule (which is typically predominantly electronic in origin) is not constant, but depends on the internuclear distance according to the equation:

$$\alpha(t) = \alpha_0 + \left(\frac{\partial \alpha}{\partial q} \right)_0 q(t) \quad (4)$$

This quantity is a tensor, but to simplify the discussion we will consider it as a scalar. Here α_0 is the polarizability of a molecule in which the internuclear distance is held at its equilibrium value.

Starting from Eqs. (4) and (5), we obtain

$$-\omega^2 q(\Omega) - 2i\omega\gamma q(\Omega) + \omega_0^2 q(\Omega) = \frac{1}{m} \left(\frac{\partial \alpha}{\partial t} \right)_0 E_P E_S^* \quad (5)$$

where m represents the reduced nuclear mass and $\Omega = \omega_P - \omega_S$. This equation shows explicitly $q(\Omega)$ as a material excitation resonantly driven by optical mixing $E_P E_S^*$. SRS by phonons can therefore be considered a result of coupling three waves E_P , E_S and $q(\Omega)$ governed by the wave equations (3) and (6). This system is essentially the wave equation coupled to an oscillator equation. Starting from Eq. (6) it is possible to calculate the resonant Raman susceptibility, which, for the steady-state case, is related to the Raman gain by the following relation:

$$g = \frac{4\pi\omega_0^2}{c^2 k^2} \text{Im}(\chi_S^{(3)R}) \quad (6)$$

When the depletion of the pump field $|E_P|^2$ is negligible, being the Raman susceptibility $\chi^{(3)R}$ a negative imaginary, we find that the evolution of the intensity of Stokes field is given by the exponentially growing solution of

$$|E_S|^2 = |E_S(0)|^2 \exp(g * |E_P|^2 * z - \alpha * z) \quad (7)$$

The Stokes wave is amplified if the gain exceeds the losses. We note that Raman amplification is a process for which the phase matching condition is automatically satisfied. In other words, Raman amplification is a pure gain process.

A.2 Experiment: measurements of Raman gain

A.2.1 Direct measurement

The theory developed in previous paragraph is a theory of Raman amplification. This means that to measure Raman gain, we should perform experiments on Raman amplifiers [47, 48]. Several materials, such as silicon, allow a direct measurement of SRS [49, 50]. In this case the Raman gain can be evaluated by measuring the Stokes amplification in a Raman amplifier having as active medium the material under test [2].

In the steady-state (no pump depletion) regime of SRS, assuming no losses at the Stokes frequency, the value of the gain coefficient g can be obtained by fitting Eq. (8), which is readily transformed into:

$$\text{SRS Gain} = 10 * \log_{10} \left(\frac{I_S(L)}{I_S(0)} \right) = 4.34 * g * L * I_P(0) \quad (8)$$

where $I_S(0)$ is the intensity of the input Stokes radiation (Stokes seed), $I_S(L)$ is the intensity of the output Stokes radiation, $I_P(0) = \frac{P}{A}$ is the intensity of the input pump radiation, P is the power incident onto the sample, A as the effective area of pump beam and L is the effective length. Since the sample is transparent to the incident light, L is taken to be equal to the thickness of the sample along the path of the incident light.

As an example, in **Figure 5** a typical trend of the maxima of the signal power plotted as a function of the effective pump power at the exit of Raman amplifier is reported. As the laser power increases, the SRS gain is first constant and then grows approximately linear when the power is greater than the threshold value and so stimulated scattering begins to prevail. The threshold is usually defined as the power at which the linear behavior starts, while the slope of the line is proportional to the Raman gain coefficient g . The estimation of the Raman gain coefficient g is not straightforward due to the uncertainty in the effective focal volume inside the sample [36, 39, 42].

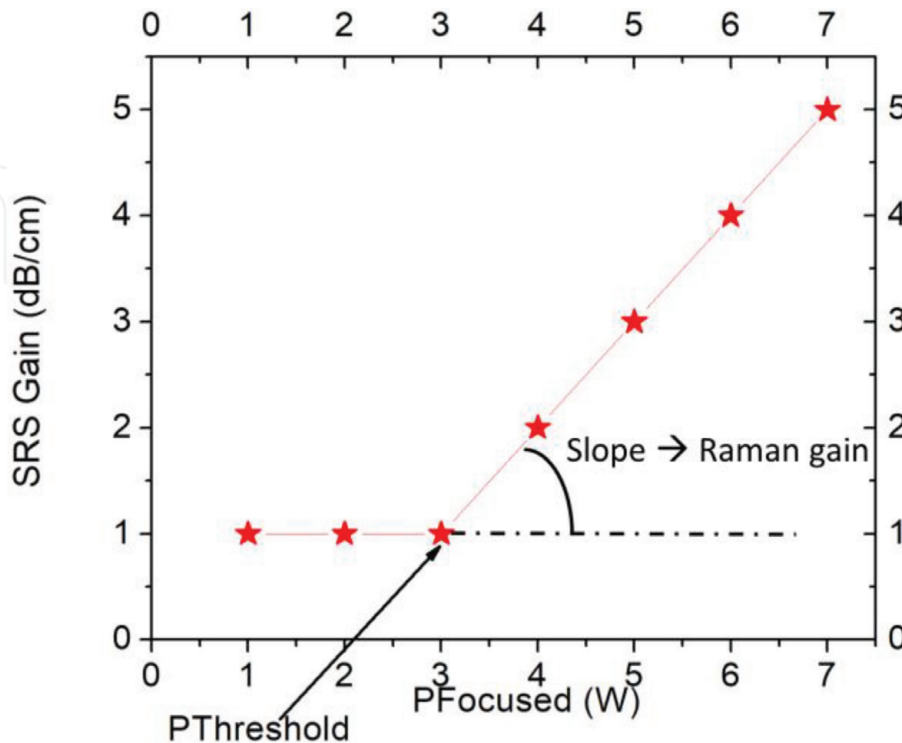


Figure 5.
A typical trend of SRS signal plotted as a function of the effective pump power.

A.2.2 Indirect measurement

If Raman gain is weak and the length of sample is small, Raman amplification is difficult to measure and an indirect measurement should be implemented. Frequently, this happens for glasses, for which the spontaneous Raman spectra is firstly measured by a standard Raman set up, then the Raman gain is estimated by a numerical procedure [2].

In order to eliminate in the measured Stokes Raman intensity $I(\omega)$ its dependence on both the temperature and the frequency of the vibrational modes [51, 52], the following relation can be used:

$$R(\omega_S) = \frac{\omega_S}{[N(\omega_S, T) + 1] (\omega_P - \omega)^4} I(\omega_S) \quad (9)$$

where ω_S is the Stokes Raman shift (in cm^{-1} units), ω_P is the laser excitation frequency, $N(\omega_S, T)$ is the Bose-Einstein mean occupation number and T is the temperature [31]. Afterwards, with the aim to properly relate the Raman spectra of investigated glasses with the standard silica glass, the measured Raman spectra can be adjusted also for the differences in reflection and angle of collection [26, 27, 31]. The relation between Raman gain spectrum and spectral and differential Raman cross section is expressed by the following equation:

$$g(\omega_S) = \frac{\lambda_S^3}{c^2 h n^2} \left(\frac{\partial^2 \sigma}{\partial \Omega \partial \omega_S} \right)_0 \quad (10)$$

where $\left(\frac{\partial^2 \sigma}{\partial \Omega \partial \omega_S} \right)_0$ is the Raman cross section at $T = 0$ K (i.e., corrected considering the thermal population factor), λ_S is the Stokes wavelength (in m), c is the velocity of light in vacuum and n is the refraction index at the excitation wavelength [24–27, 31].

Conflict of interest

The authors declare that they have no competing financial interests.

Author details

Maria Antonietta Ferrara* and Luigi Sirleto
National Research Council (CNR), Institute for Microelectronics and Microsystems (IMM), Napoli, Italy

*Address all correspondence to: antonella.ferrara@na.imm.cnr.it

IntechOpen

© 2018 The Author(s). Licensee IntechOpen. This chapter is distributed under the terms of the Creative Commons Attribution License (<http://creativecommons.org/licenses/by/3.0>), which permits unrestricted use, distribution, and reproduction in any medium, provided the original work is properly cited. 

References

- [1] Popp J, Kiefer W. Raman scattering. In: Meyers RA, editor. *Fundamentals, Encyclopedia of Analytical Chemistry*. Chichester: John Wiley & Song Ltd; 2000. pp. 13104-13142
- [2] Sirleto L, Vergara A, Ferrara MA. Advances in stimulated Raman scattering in nanostructures. *Advances in Optics and Photonics*. 2017;**9**(1): 169-217. DOI: 10.1364/AOP.9.000169
- [3] Cern P, Jelinkov H, Zverevb PG, Basiev TT. Solid state lasers with Raman frequency conversion. *Progress in Quantum Electronics*. 2004;**28**:113
- [4] Stolen RH. In: Islam MN, editor. *Raman Amplifiers for Telecommunications 1*. New York: Springer-Verlag; 2004. p. 35
- [5] Rivero C, Richardson K, Stegeman R, Stegeman G, Cardinal T, Fargin E, et al. Quantifying Raman gain coefficients in tellurite glasses. *Journal of Non-Crystalline Solids*. 2004;**345** & **346**:396-401
- [6] Liang D, Bowers JE. Recent progress in lasers on silicon. *Nature Photonics*. 2010;**4**:511. DOI: 10.1038/nphoton.2010.167
- [7] Boyraz O, Jalali B. Demonstration of a silicon Raman laser. *Optics Express*. 2004;**12**:5269
- [8] Rong HS, Liu A, Jones R, Cohen O, Hak D, Nicolaescu R, et al. An all-silicon Raman laser. *Nature*. 2005;**433**:292
- [9] Wiersma DS. Disordered photonics. *Nature Photonics*. 2013;**7**:188
- [10] Lin H-B, Campillo AJ. Microcavity enhanced Raman gain. *Optics Communication*. 1997;**133**:287
- [11] Spillane SM, Kippenberg TJ, Vahala KJ. Ultralow-threshold Raman laser using a spherical dielectric microcavity. *Nature*. 2002;**415**:621-623
- [12] Latawiec P, Venkataraman V, Burek MJ, Hausmann BJM, Bulu I, Lončar M. On-chip diamond Raman laser. *Optica*. 2015;**2**:924. DOI: 10.1364/OPTICA.2.000924
- [13] Takahashi Y, Inui Y, Chihara M, Asano T, Terawaki R, Noda S. A micrometre-scale Raman silicon laser with a microwatt threshold. *Nature*. 2013;**498**:470-474
- [14] Schuurmans FJP, Vanmaekelbergh D, van de Lagemaat J, Lagendijk A. Strongly photonic macroporous GaP networks. *Science*. 1999;**284**:141
- [15] Hokr BH, Bixler JN, Cone MT, Mason JD, Beier HT, Noojin GD, et al. Bright emission from a random Raman laser. *Nature Communications*. 2014;**5**:4356. DOI: 10.1038/ncomms5356
- [16] Zheludev NI. Nonlinear optics on the nanoscale. *Contemporary Physics*. 2002;**43**:365. DOI: 10.1080/00107510110102281
- [17] Banfi G, De Giorgio V, Ricard D. Nonlinear optical properties of semiconductor nanocrystals. *Advances in Physics*. 1998;**47**:447
- [18] Suresh S, Arivuoli D. Nanomaterials for nonlinear optical applications: A review. *Reviews on Advanced Materials Science*. 2012;**30**:243-253
- [19] Chandra M, Das PK. Small-particle limit in the second harmonic generation from noble metal nanoparticles. *Chemical Physics*. 2009;**358**:203. DOI: 10.1016/j.chemphys.2009.02.003
- [20] Kawata S, Inouye Y, Verma P. Plasmonics for near-field nano-imaging and superlensing. *Nature Photonics*. 2009;**3**:388

- [21] Vildirim H, Bulutay C. Enhancement of optical switching parameter and third-order optical nonlinearities in embedded Si nanocrystals: A theoretical assessment. *Optics Communication*. 2008;**281**:4118
- [22] Zhang BP, Shimazaki K, Shiokawa T, Suzuki M, Ishibashi K, Saito R. Stimulated Raman scattering from individual single-wall carbon nanotubes. *Applied Physics Letters*. 2006;**88**(24):241101-241103
- [23] Wu J, Gupta AK, Gutierrez HR, Eklund PC. Cavity-enhanced stimulated Raman scattering from short GaP nanowires. *Nano Letters*. 2009;**9**(9):3252-3257
- [24] Galeener FL, Mikkelsen JC Jr, Geils RH, Mosby WJ. The relative Raman cross sections of vitreous SiO₂, GeO₂, B₂O₃, and P₂O₅. *Applied Physics Letters*. 1978;**32**:34-36
- [25] Irannejad M, Jose G, Jha A, Steenson P. Raman gain in modified tellurite glasses and thin films. *Optics Communication*. 2012;**285**:2646-2649
- [26] Manikandan N, Rysanyanskiy A, Toulouse J. Thermal and optical properties of TeO₂-ZnO-BaO glasses. *Journal of Non-Crystalline Solids*. 2012;**358**:947-951
- [27] Lin A, Rysanyansky A, Toulouse J. Fabrication and characterization of a water-free mid-infrared fluorotellurite glass. *Optics Letters*. 2011;**36**:740-742
- [28] Sirleto L, Donato MG, Messina G, Santangelo S, Lipovskii AA, Tagantsev DK, et al. Raman gain in niobium-phosphate glasses. *Applied Physics Letters*. 2009;**94**:031105. DOI: 10.1063/1.3072354
- [29] Donato MG, Gagliardi M, Sirleto L, Messina G, Lipovskii AA, Tagantsev DK, et al. Raman optical amplification properties of sodium–niobium–phosphate glasses. *Applied Physics Letters*. 2010;**97**:231111. DOI: 10.1063/1.3525162
- [30] Ferrara MA, D'Arco A, Indolfi M, Sirleto L. Stimulated Raman scattering in nanostructured materials. In: *IEEE 15th International Conference on Nanotechnology (IEEE-NANO)*. 2015
- [31] Pernice P, Sirleto L, Vergara A, Aronne A, Gagliardi M, Fanelli E, et al. Large Raman gain in a stable nanocomposite based on niobiosilicate glass. *Journal of Physical Chemistry C*. 2011;**115**(35):17314-17319. DOI: 10.1021/jp204353e
- [32] Sirleto L, Aronne A, Giofrè M, Fanelli E, Righini GC, Pernice P, et al. Compositional and thermal treatment effects on Raman gain and bandwidth in nanostructured silica based glasses. *Optical Materials*. 2013;**36**:408-413. DOI: 10.1016/j.optmat.2013.10.001
- [33] Sirleto L, Raghunathan V, Rossi A, Jalali B. Raman emission in porous silicon at 1.54 μm. *Electronics Letters*. 2004;**40**(19):121-122. DOI: 10.1049/el:20045284
- [34] Sirleto L, Ferrara MA, Rendina I, Jalali B. Broadening and tuning of spontaneous Raman emission in porous silicon at 1.5 μm. *Applied Physics Letters*. 2006;**88**:211105. DOI: 10.1063/1.2206123
- [35] Ferrara MA, Donato MG, Sirleto L, Messina G, Santangelo S, Rendina I. Study of strain and wetting phenomena in porous silicon by Raman scattering. *Journal of Raman Spectroscopy*. 2008;**39**(2):199-204. DOI: 10.1002/jrs.1846
- [36] Sirleto L, Ferrara MA, Rendina I, Nicotra G, Spinella C. Observation of stimulated Raman scattering in silicon nanocomposites. *Applied Physics Letters*. 2009;**94**:221106. DOI: 10.1063/1.3148669

- [37] Ferrara MA, Sirleto L, Nicotra G, Spinella C, Rendina I. Enhanced gain coefficient in Raman amplifier based on silicon nanocomposites. *Photonics and Nanostructures—Fundamentals and Applications*. 2011;**9**:1-7. DOI: 10.1016/j.photonics.2010.07.007
- [38] Sirleto L, Ferrara MA, Rendina I, Basu SN, Warga J, Li R, et al. Enhanced stimulated Raman scattering in silicon nanocrystals embedded in silicon-rich nitride/silicon superlattice structures. *Applied Physics Letters*. 2008;**93**:251104. DOI: 10.1063/1.3050109
- [39] Ferrara MA, Rendina I, Basu SN, Dal Negro L, Sirleto L. Raman amplifier based on amorphous silicon nanoparticles. *International Journal of Photoenergy*. 2012;**2012**:254946. DOI: 10.1155/2012/254946
- [40] Ferrara MA, Sirleto L. Experimental investigation of stimulated Raman scattering gain in silicon nanocomposite and in amorphous silicon nanoparticles. *Journal of Nonlinear Optical Physics and Materials*. 2012;**21**(3):1250039. DOI: 10.1142/S0218863512500397
- [41] Ferrara MA, D'Arco A, Indolfi M, Sirleto L. Study of Raman amplification in nanostructured materials. In: *AEIT International Annual Conference, IEEE Proceeding*. Article number 7415223. 2015. DOI: 10.1109/AEIT.2015.7415223
- [42] Sirleto L, Ferrara MA, Nikitin T, Novikov S, Khriachtchev L. Giant Raman gain in silicon nanocrystals. *Nature Communications*. 2012;**3**:1220. DOI: 10.1038/ncomms2188
- [43] Sirleto L, Ferrara MA, Vergara A. Toward an ideal nanomaterial for on-chip Raman laser. *Journal of Nonlinear Optical Physics and Materials*. 2017;**26**:1750039. DOI: 10.1142/S0218863517500394
- [44] Boyd RW. *Nonlinear Optics*. 2nd ed. USA: Academic Press; 2003
- [45] Shen YR. *The Principles of Nonlinear Optics*. New York: John Wiley & Sons, Inc; 2003
- [46] Yariv A. *Quantum Electronics*. New York: John Wiley & Sons, Inc; 1988
- [47] Levine BF, Shank CV, Heritage JP. Surface vibrational spectroscopy using stimulated Raman scattering. *IEEE Journal of Quantum Electronics*. 1979;**15**:1418
- [48] Levine BF, Bethea CG. Ultrahigh sensitivity stimulated Raman gain spectroscopy. *IEEE Journal of Quantum Electronics*. 1980;**16**:85
- [49] Ralston JM, Chang RK. Spontaneous Raman scattering efficiency and stimulated scattering in silicon. *Physical Review B*. 1970;**2**:1858
- [50] Owyong A. Sensitivity limitations for cw stimulated Raman spectroscopy. *Optics Communication*. 1977;**22**:323
- [51] Shuker R, Gammon RW. Raman-scattering selection-rule breaking and the density of states in amorphous materials. *Physical Review Letters*. 1970;**25**:222
- [52] Galeener FL, Sen PN. Theory for the first-order vibrational spectra of disordered solids. *Physical Review B*. 1978;**17**:1928